Reaction Kinetics And Simulation Of Nonivamide Batch Reaction

Zhaoyi Xing, Zhiyun Zou*, and Xinhong Liu

State Key Laboratory of Chemistry for NBC Hazards Protection, Beijing 102205, China

Corresponding author. E-mail: zhiyunzouzzy@outlook.com

Received: Dec. 08, 2025; Accepted: Feb. 18, 2026

The nonivamide batch reaction process primarily relies on empirical production knowledge, with a notable absence of systematic research. This study for the first time systematically investigates the reaction kinetics of nonivamide synthesis by integrates experimental methods, employing the RC1e calorimeter to ensure reaction safety, and investigates the reaction kinetics of capsaicin synthesis. It innovatively combines the RC1e calorimeter and Aspen Plus software to carry out reaction safety evaluation and process parameter optimization : it uses the Aspen Plus software, incorporating the NRTL thermodynamic model, to simulate the batch reaction stages and conduct dynamic simulations. The study validates the reliability of kinetic equations derived from these simulations. It also examines the impacts of the reactant molar ratio (The molar ratio referred to below indicates $C_9H_{17}ClO : C_8H_{12}ClNO_2$), feed temperature, and feed rate on product yield, leading to the optimization of operational parameters. The results reveal that at 40°C, the reaction rate constant for this synthesis process is 0.1486 $L/(mol \cdot s)$, with the kinetic equation expressed as $k = 34960.37e^{\frac{-100911}{RT}}$. In terms of optimizing product yield, the findings indicate that a reactant molar ratio of 1.1:1 enhances the yield by 1.934 percentage points; a feed temperature of 38°C improves the yield by 1.889 percentage points; and maintaining a feed duration of 60 minutes further increases the yield by 0.055 percentage points, building on the optimized temperature conditions. The optimized parameters can realize a stable increase of 3.878 percentage points in the yield of industrial nonivamide production, control the adiabatic temperature rise below 11.415°C, and reduce the load of the reactor cooling system by about 15%, which provides reliable kinetic models and engineering operation parameters for the industrial scale-up of nonivamide synthesis and solves the engineering problems of yield fluctuation and high safety risk caused by empirical operation.

Keywords: Nonivamide; batch reaction; reaction kinetics; calorimetry; Aspen Plus; process scale-up; liquid-liquid two-phase reaction

http://dx.doi.org/10.6180/jase.202608_31.065

1. Introduction

Nonivamide, a synthetic analog of capsaicin, presents as a pungent white powder and shares similar bioactivity with its natural counterpart. It finds extensive application in the fields of pharmaceuticals, pesticides, biological research, food additives (flavor enhancers) and security repellents ; the global market demand for synthetic capsaicin products represented by nonivamide is increasing at an annual rate of about 8%, and the industrial synthesis of Nonivamide typically involves a batch reaction process using Vanillylamine hydrochloride and sodium bicarbonate as substrates, with nonanoyl chloride serving as the reactant. This reaction, which is both rapid and exothermic, culminates in multiple physical stages including filtration and crystallization to yield the final product [1]. The exothermic nature of this synthesis imposes significant challenges in ensuring operational safety and achieving high yields, and is currently under-researched in terms of systematic

reaction kinetics. The transition from laboratory-scale production to industrial-scale manufacturing mandates the development and application of kinetic models to optimize process conditions [2].

Current research in the domain of rapid exothermic batch reactions primarily focuses on process optimization through simulation. For instance, Li Delun et al. enhanced the yield of bisphenol A and the conversion rate of acetone by 3.96% and 4.30% respectively in a bisphenol A production facility through reaction unit optimization. Similarly, Li Mujin et al. employed simulation techniques to optimize the HPPO epoxy reaction in a tubular fixed-bed reactor, developing a model to investigate the factors affecting bed hotspot temperatures via sensitivity analysis. Other processes, such as those occurring in atmospheric and dehydration towers, have also been refined using Aspen Plus software, where the technology has reached a level of maturity. Despite these advancements, no comprehensive studies have been conducted on the synthesis reaction of Nonivamide. This study represents the first systematic investigation into the kinetics of Nonivamide synthesis, establishing a reaction mechanism and deriving kinetic equations. Additionally, the use of an RC1e calorimeter to measure the reaction heat contributes to ensuring the safety of the production process. A process simulation system was developed to dynamically simulate the Nonivamide synthesis reaction and validate the reliability of the kinetic parameters. This validation was performed through comparative analysis of small-scale laboratory experiments, RC1e scale-up experiments, and simulated results, thereby optimizing operational parameters to support industrial scale-up. Different from the existing simulation studies focusing on single homogeneous phase or non- S_N2 type reaction systems, this study targets the characteristics of nonivamide liquid-liquid two-phase S_N2 rapid exothermic reaction, for the first time realizing the integrated research of reaction kinetics modeling, thermal safety assessment and process dynamic simulation, and filling the research gap of nonivamide synthesis industrial scale-up theory [3].

2. Materials and methods

2.1. Batch Reaction Experiments

In the laboratory, small-scale batch experiments for Nonivamide synthesis are conducted by varying the quantities of reactants to study the influence of operational conditions on reaction efficiency. The concentration of the product is determined using the gas chromatography external standard method. Product concentrations from multiple experimental samples are calculated using a standardized calibration equation to establish a reaction kinetics model.

The principal reaction equation is presented as follows:

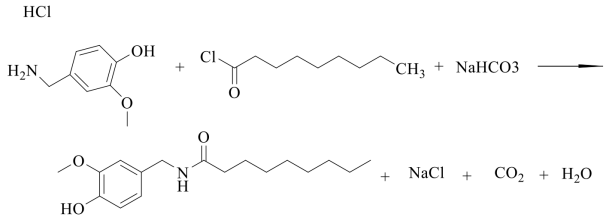

Fig. 1. The principal reaction equation for Nonivamide synthesis

2.1.1. *Experimental Reagents and Materials*

Vanillylamine hydrochloride ($C_8H_{12}ClNO_2$, 99%), nonanoyl chloride ($C_9H_{17}ClO$, 95%), sodium bicarbonate ($NaHCO_3$, 99.8%), and dichloromethane (CH_2Cl_2, 99.5%) were procured from Shanghai Macklin Biochemical Co., Ltd.

2.1.2. *Batch Reaction Small-Scale Experiment Apparatus*

The experimental setup comprised a 250 mL jacketed three-neck flask employed as the primary reaction vessel. The flask was connected to a constant temperature water bath that circulated water through the jacket, serving as a heat exchange medium. This arrangement was crucial for minimizing temperature discrepancies between the set and actual values, thus facilitating effective heat exchange and the prompt dissipation of heat generated during the rapid exothermic batch reactions. The apparatus was equipped with a constant-pressure dropping funnel to facilitate the controlled addition of reactant solutions, a middle condenser to maintain solvent reflux post-temperature rise, and a thermometer to monitor internal reaction temperatures. A magnetic stirrer was utilized to maintain a homogeneous and suspended state of the reaction mixture.

2.1.3. *Investigation of the Impact of Reactant Quantities*

A series of batch synthesis reactions were performed to gather empirical data. The experiments focused on varying the quantities of reactants to evaluate the effects of scaling the reaction. Collecting numerous data sets was essential for the development of a reaction kinetics model.

Experimental Procedure:

- **Step 1:** $C_8H_{12}ClNO_2$ and $NaHCO_3$ were dissolved in a mixture of CH_2Cl_2 and water. The solution was transferred to a 250 mL jacketed three-neck flask. Due to the limited solubility of $C_8H_{12}ClNO_2$, the beaker and flask walls were rinsed with a small volume of water to prevent residual material loss.

- **Step 2:** $C_9H_{17}ClO$ was dissolved in CH_2Cl_2 to prepare Solution B, which was transferred to a constant-pressure dropping funnel. The solution was gradually added to the three-neck flask.

- **Step 3:** During addition, the reaction temperature was maintained below 25°C. After complete addition, the temperature was raised to 40°C and the mixture was refluxed for 2–3 hours.

- **Step 4:** Upon completion, the aqueous phase was separated and discarded, while the organic phase was retained. The organic layer was washed twice with water, followed by evaporation of CH_2Cl_2. Ethanol was added to dissolve the residue completely. A sodium hydroxide solution in ethanol was then added slowly under cooling at approximately 0°C. The product was allowed to crystallize, filtered, and dried to obtain the final solid.

As the reaction progressed, occasional occurrences of suspended solids or stratification were observed within the three-neck flask. Consequently, maintaining high-speed stirring was essential to ensure thorough contact among the reactants [4].

Upon completion of the reaction, a 0.2 mL sample was extracted using a pipette and transferred into a sample vial, which was then diluted to 1.5 mL with methanol. This procedure ensures that the dilution level can be precisely calculated while significantly diluting any unreacted reactants. Such dilution effectively quenches the reaction by rendering it impossible for the reaction to proceed at extremely low concentrations. Subsequently, the samples were analyzed using GC-MS.

The experimental procedure was then repeated under altered conditions, with each batch synthesis reaction's condition data presented in Table 1.

Each group of reactants in this experiment is fed at an equimolar ratio, and the influence of reaction scale on the reaction result is investigated only through equal proportion scaling of the material amount.

The experimental results suggest that reducing the quantity of reactants enhances the reaction outcome. It is hypothesized that a lesser volume of materials, when subjected to fixed magnetic stirring, facilitates better mixing, thereby allowing for more thorough interaction among the reactants. Conversely, when the volume of materials is increased, the reaction system often appears as a suspension. This requires maintaining a certain stirring speed to prevent solid precipitation. It is speculated that sustaining appropriate stirring efficiency with increased quantities of materials can stabilize the reaction rate and mitigate the effects of scaleup [[5].

2.1.4. Investigation of the Impact of Stirring Rate

Based on preliminary experiments, it is hypothesized that the stirring rate significantly influences the outcomes of the synthesis process. To mitigate the effects of extraneous variables, a series of controlled experiments was conducted with progressively increasing stirring rates. This approach aimed to ascertain the maximum stirring rate that does not adversely affect the reaction outcome. The experimental conditions were as follows: Solution A comprised 0.005 mol of vanillylamine, 1.083g of $NaHCO_3$, 15 mL of CH_2Cl_2, and 50 mL of water; Solution B contained 0.005 mol of $C_9H_{17}ClO$ and 15 mL of CH_2Cl_2 . The stirring rates tested were 800 , 1000, 1200, 1300, and 1400 rpm . The results demonstrate that stirring rates exceeding 1300 rpm do not further influence the reaction outcome [6].

2.1.5. Investigation of the Impact of Reaction Temperature

With the stirring rate fixed at 1300 rpm , the influence of reaction temperature on the synthesis was explored through a series of experiments. Samples were collected immediately after the completion of reactant addition, and subsequently at 30 minutes, 1 hour, 1.5 hours, and 2 hours, each diluted to 1.5 ml with methanol for GC-MS analysis. The reaction exhibited minimal progress at 25°C, which is significant given the boiling point of CH_2Cl_2, the solvent used, at 39.6°C. Consequently, the experimental temperatures were varied between 25°C and 40°C. The experimental setup included Solution A with the same composition as previously described, and Solution B also remained consistent. The temperatures tested were 25, 28, 31, 34, 37, and 40°C. Three trials were conducted under each set of conditions, and the results were averaged. Findings from these experiments clearly indicate that the reaction temperature profoundly affects the reaction rate, with a notable decrease in rate observed as the temperature decreases.

2.1.6. External Standard Calibration

In the realm of gas chromatography, samples introduced into a chromatographic column undergo gas-solid partitioning. This process facilitates the separation of components due to their differing solubility and desorption properties between the mobile and stationary phases. Detection of these components is primarily conducted using an FID, where qualitative analysis is executed with standard samples and quantitative analysis is performed through external standard calibration.

Table 1. Experimental condition data for investigation of the impact of reactant quantities (equal proportion scaling)

Experiment serial number	Solution A				Solution B		Temperature (°C)
	$C_8H_{12}ClNO_2$ (mol)	$NaHCO_3$ (g)	CH_2Cl_2 (ml)	H_2O (ml)	$C_9H_{17}ClO$ (mol)	CH_2Cl_2 (ml)	
1	0.03	6.5	30	100	0.03	30	40
2	0.027	5.85	27	90	0.027	27	40
3	0.024	5.2	24	80	0.024	24	40
4	0.021	4.55	21	70	0.021	21	40
5	0.018	3.9	18	60	0.018	18	40
6	0.015	3.25	15	50	0.015	15	40

2.1.7. *Establishing a Standard Curve*

To create a standard curve, a precisely measured 0.4 g of Nonivamide standard is dissolved in methanol to a total volume of 50 ml in a volumetric flask, forming the stock solution. From this stock solution, aliquots of 2.5ml, 10ml, and 25 ml are further diluted to 50 ml to establish a series of dilution concentrations. Subsequently, 1.5 ml from each diluted solution is analyzed via gas chromatography to construct the standard curve. The concentrations prepared are 0.4 mg/ml, 1.6mg/ml, 4mg/ml, and 8mg/ml, respectively. Typically, the relationship between the peak area and concentration in gas chromatography is linear. This linear relationship is graphically represented with concentration on the abscissa and peak area on the ordinate, yielding a linear equation of the form $y = kx + b$, where y denotes the peak area, x denotes concentration, and k and b are the slope and intercept, respectively.

Analysis of the product typically shows elution times between 14.60 and 14.80 minutes. From the calibration curve, a linear equation $y = 1.199 \times 10^7 x - 1.834 \times 10^7$ is derived, best fitting the four data points with an adjusted $R^2 = 1$.

2.1.8. *Analyzing Test Samples and Calculating Concentration*

For the analysis of experimental samples, 0.2 ml of the experimental product solution is diluted to 1.5 ml with methanol and subjected to gas chromatography analysis. The retention time and peak area of the product components in the test sample are recorded. The concentration of the product is then calculated using the peak area and the previously established standard curve equation from the external calibration [7].

The experimental data indicate that the change in peak area over time is minimal, suggesting that most of the reaction occurs rapidly within the initial hour, with negligible further reaction thereafter. Even two hours later, some reactants remain unreacted, indicative of a predominantly second-order reaction kinetics, consistent with the observed results.

2.2. RC1e Process Scale-Up Experiment

This study utilized an RC1e calorimetric reactor, furnished with a 2 -liter atmospheric pressure glass reactor, to conduct scale-up experiments for the synthesis of Nonivamide. The primary objective was to quantify the heat release and gather thermochemical data, including exothermic characteristics, rate of heat release, and total reaction heat. Given the reactor's 2liter capacity, it was essential to maintain a minimum reactant volume of 1.2 L to ensure optimal performance of the stirring mechanism and temperature measurement functionalities. The procedural parameters recorded during the reaction are depicted in Fig. 5.

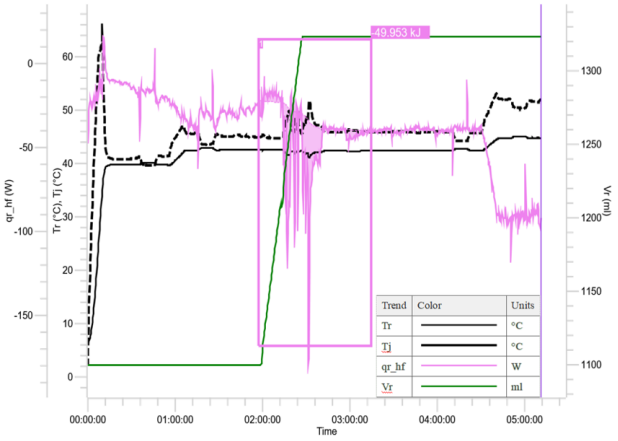

Fig. 2. Overall trend of the experiment

In Fig. 2, the variables are denoted as follows: Tr represents the internal temperature of the reactor, Tj signifies the jacket temperature, qr indicates the heat release, Vr denotes the volume of the reactor's solution, and Time is expressed in hours, minutes, and seconds. The specific heat capacity of the mixture within the reactor system was measured both prior to and following the reaction [8].

Subsequent to calibration adjustments, the total heat released during the reaction phase was determined to be 49.953 kJ . Consequently, the molar heat of reaction (ΔHm) was calculated as 249.765 kJ/mol, derived from the ratio

of total heat released to the amount of substance reacted (49.953 kJ/0.2 mol).

Analysis of the volume curve (Vr) revealed clear demarcations for the initiation and completion of reactant addition. Notably, a significant exothermic response was observed at the onset of reactant addition, leading to a rapid increase in the reactor's internal temperature (Tr). This necessitated swift intervention via the temperature control system to cool the jacket temperature (Tj), after which the temperature gradually achieved stability. The adiabatic temperature rise (ΔT_{ad}) was calculated to be 11.415 . According to the Code for Safety Design of Chemical Process (GB 50160-2018), the severity of uncontrolled exothermic reaction is negligible when the adiabatic temperature rise is less than 20°C, which belongs to low safety risk. Under these specific concentration conditions and based on the severity criteria for uncontrolled exothermic reactions, the severity of the uncontrolled heat release during the Nonivamide synthesis was deemed negligible [9].

Following the completion of reactant addition, there was a marked decline in the rate of heat release, indicating that the reaction dynamics were primarily controlled by the rate of reactant addition. This is consistent with findings from previous studies indicating that the reaction is exothermic. Examination of the graphical data suggests that most of the reactants had fully reacted by the end of the addition phase.

To further explore the impact of reaction temperature on the process, the experiment was repeated with adjustments to the reaction temperatures. Specifically, the reaction temperatures were set at 28°C, 31°C, 34°C, 37°C, and 40°C across five separate trials.

2.3. Kinetic Modeling

The synthesis of Nonivamide proceeds via a mechanism analogous to the S_N2 reaction, involving $C_8H_{12}ClNO_2$ as the substrate and $C_9H_{17}ClO$ as the nucleophilic reagent. The kinetic rate expression for the rate-determining step correlates with the concentrations of these reactants [10, 11]:

$$\mathrm{r} = \mathrm{k}[\mathrm{RX}][\mathrm{Nu}] \tag{1}$$

In Eq. (1), [RX] and [Nu] denote the concentrations of $C_8H_{12}ClNO_2$ and $C_9H_{17}ClO$ at time t , respectively.

Let x represent the quantity of product formed during time t , initially set to zero.

$$\frac{dx}{dt} = k\left([RX]_0 - x\right)\left([Nu]_0 - x\right) \tag{2}$$

Eq. (2) introduces $[RX]_0$ and $[Nu]_0$ as the initial concentrations of $C_8H_{12}ClNO_2$ and $C_9H_{17}ClO$, respectively. In all conducted experiments, these initial concentrations were equivalent, and given the stoichiometry of the reaction where the stoichiometric coefficients for both reactants are 1 , this simplifies the Eq. (3) [12, 13]:

$$\frac{d[RX]}{dt} = -k[RX]^2 \tag{3}$$

The S_N2 reaction typifies a second-order reaction, and integration of the reaction equation provides:

$$\frac{1}{[RX]_0 - x} - \frac{1}{[RX]_0} = kt \tag{4}$$

Experimental observations, such as those from RC1e calorimeter experiments at 40°C, reveal temporal changes in product concentration, as documented in Table 2.

A linear regression analysis yields $y = 0.1637x + 1.9307$ with an adjusted $R^2 = 0.8756$, as illustrated in Fig. 3. The inverse concentration of the substrate, $\frac{1}{[RX]}$, exhibits a linear relationship with time t, confirming the second-order reaction behavior. The intercept approximates $\frac{1}{[RX]_0} = 2$, while the slope represents the reaction rate constant $k = 0.1637$.

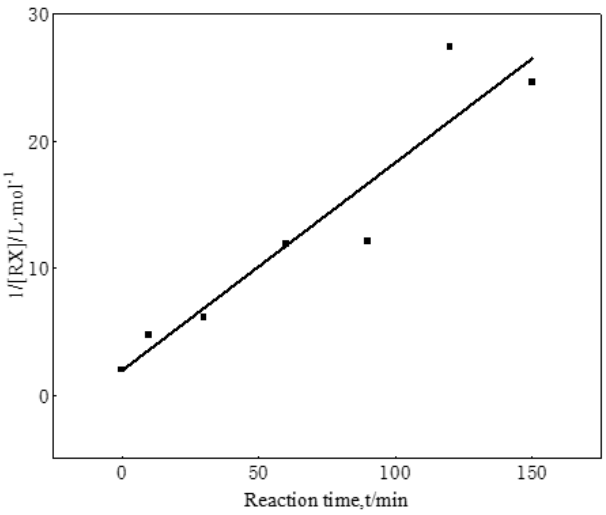

Fig. 3. Laboratory experiment $\frac{1}{[RX]}$ fits the equation with the reaction time t

Utilizing the derived formulas, the reaction rate constants at varying temperatures are calculated using the Arrhenius equation to establish the temperature-dependence of the reaction rate:

$$\mathrm{k} = \mathrm{Ae}^{\frac{-\mathrm{Ea}}{\mathrm{RT}}} \tag{5}$$

The temperature-dependent reaction rate constants from both small-scale and scale-up experiments are presented in Table 3 and Table 4, respectively.

Table 2. Variation of product concentration over time

Time t (min)	0	30	60	90	120	150
Product concentration (mol L^{-1})	0	0.336	0.416	0.417	0.463	0.459

Table 3. Reaction rate constants from small-scale laboratory experiments across temperatures

Temperature (K)	298	301	304	307	310	313
Rate constant (L/(mol·s))	0.0828	0.0906	0.1074	0.1160	0.1373	0.1637

Using 1/T as the abscissa and lnk as the ordinate, the fitting of a linear equation $y = -4200.1x + 11.573$ results in an adjusted $R^2 = 0.9808$, depicted in Fig. 4.

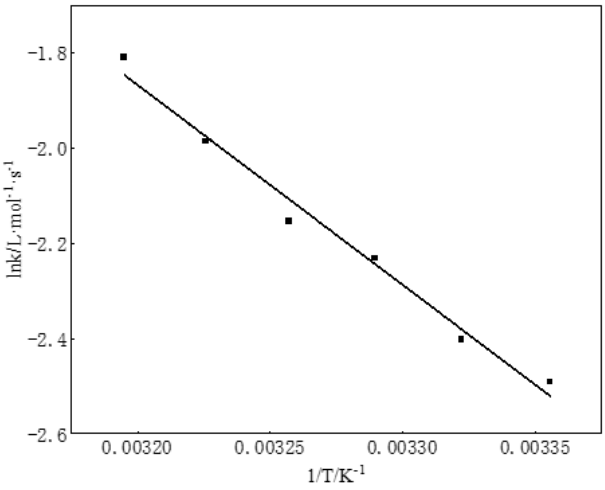

Fig. 4. Laboratory experiments lnk with $\frac{1}{T}$ fitting equations

The slope of the equation is $-\frac{E_a}{R}$, and the intercept is $\ln(A)$; thus, the kinetic equation for the small-scale experiment is formalized:

$$k = 34919.6314e\frac{-106191}{RT} \tag{6}$$

Similarly, for the RC1e process scale-up experiment, a linear equation $y = -4205x + 11.522$ is fitted, yielding an adjusted $R^2 = 0.9981$, as shown in Fig. 5.

Consequently, the kinetic equation for the RC1e process scale-up experiment is:

$$k = 34960.37e^{\frac{-100911}{RT}} \tag{7}$$

When comparing the small-scale experiments with the RC1e process scale-up experiments, it is observed that the reaction rate constants at lower temperatures are comparable. However, at higher temperatures, the rate constants for the RC1e experiments are noticeably lower. This disparity suggests that scale-up may lead to less efficient reactions in the RC1e experiments at elevated temperatures. Despite

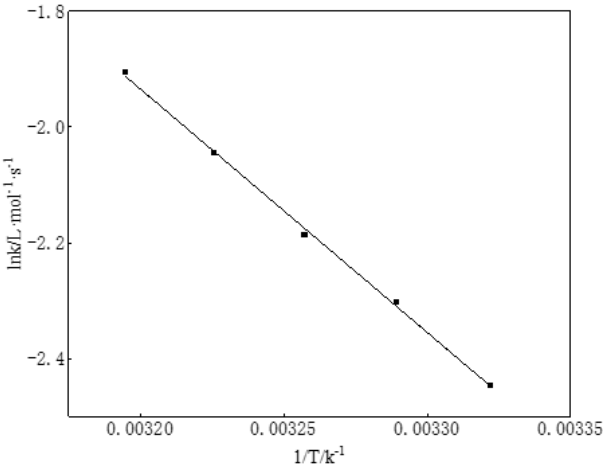

Fig. 5. RC 1 e experiment ln k fits the equation with $\frac{1}{T}$

the superior temperature control capabilities of the RC1e calorimeter, factors such as heat transfer can be excluded, shifting the focus to mass transfer effects. It is plausible that the larger volume of the reaction vessel in the scale-up experiments diminishes mass transfer efficiency. As the temperature reaches a certain threshold, the influence of temperature on the reaction's progress decreases, whereas the impact of mass transfer limitations becomes more pronounced, resulting in decreased reaction rate constants. In contrast, the small-scale experiments, which examined the effect of stirring rate on the reaction, determined that mass transfer efficiency does not significantly affect the reaction rate [14].

3. Results and discussion

3.1. Component Properties

The components involved in the Nonivamide synthesis reaction are largely available in the Aspen physical property database, as enumerated in Table 5. However, the component $C_8H_{12}ClNO_2$ is absent and has been substituted with a custom component, referred to here as Component A. The physical properties of this substitute are estimated using the Physical Property Estimation System (PCES), which requires inputs such as molecular weight, boiling point,

Table 4. Reaction rate constants from the RC1e process scale-up experiment across temperatures

Temperature T/K		301	304	307	310	313
Rate constant $(\text{mol} \cdot \text{s})$	k/L/	0.0907	0.0999	0.1122	0.1293	0.1486

vapor pressure, and molecular formula [15].

Further refinement and supplementation of missing properties in the physical property database are accomplished using the NIST TDE [16, 17]. The determined physical property parameters for the main reactants and products are detailed in Table 6.

3.2. Selection of Property Method

Given the focus on the Nonivamide synthesis reaction steps, the system is characterized by its polarity. Consequently, an activity coefficient model is deemed appropriate for this context. The operational pressure of the system is low, remaining below 10 atm , and the presence of electrolytes is negligible. Additionally, $C_8H_{12}ClNO_2$ is dissolved in CH_2Cl_2 and water, and does not participate as a solid in the reaction. Therefore, the conventional NRTL model is utilized [18].

3.3. Establishment of Steady State Model and Dynamic Model

3.3.1. Establishment of Steady State Model

A simple steady state model has been developed using Aspen software, as depicted in Fig. 6. This model's initial flow-rate data is derived by proportionally scaling up from the data obtained during the RC1e calorimeter reaction experiments.

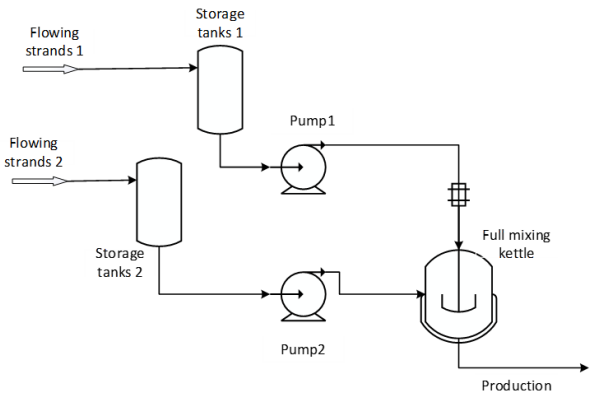

Fig. 6. Steady-state process simulation of the Nonivamide synthesis reaction

Flow-strand 1 consists of a mixture of $C_8H_{12}ClNO_2$, $NaHCO_3$, CH_2Cl_2, and water. The specific compositions of these components are detailed in Table 7.

Flow-strand 2 contains a mixture of $C_9H_{17}ClO$ and CH_2Cl_2 , with the specific components enumerated in Table 8.

Valves V1 and V2 are set to maintain atmospheric outlet pressure. The feed flow-strands are introduced at ambient temperature and pressure. Upon entering reactor C1, the temperature is adjusted to 40°C to facilitate the reaction, with flow-strand 5 serving as the reaction output. Reactor C1 functions within the BatchOp module framework, accommodating both continuous and batch feed flow-strands, thereby enabling the simulation of semi-batch reactions. This reactor operates as a kettle reactor and is indicative of a module in steady state simulation capable of representing the transient states in batch reactions [19, 20]. The reaction parameters are configured according to a power law model, incorporating reaction rate constants, preexponential factors, and activation energies derived from the RC1e experiments.

3.3.2. Dynamic Model

Building upon the foundation established by the steady-state simulation, the process flow in this dynamic model is pressure-driven and meticulously regulated. Flow controllers have been integrated to manage the operations of flow-strand 1 and flow-strand 2 . Flow-strand 1 is engineered to feed in fixed batch intervals, while flow-strand 2 maintains a consistent flow rate during the continuous input stage. During the reaction and output phases, however, the flow ceases entirely. A temperature controller is employed to maintain a constant reactor temperature, thereby emulating the precise temperature regulation achievable with an RC1e calorimeter [21, 22].

The feed duration for flow-strand 2 is set at 30 minutes, during which the primary reactants, $C_8H_{12}ClNO_2$ and $C_9H_{17}ClO$, are introduced at a concentration of 100 mol .

PID control strategies are applied to the flow rates of both flow-strands. For flow-strand

1, the thermal load of the reactor serves as an indicator of whether the reaction has commenced. Prior to the initiation of the reaction, a batch of $C_8H_{12}ClNO_2$ is added to the reactor within a predetermined timeframe. A change in the thermal load of the reactor, indicating a value other than zero, signals the onset of the reaction, prompting the PID controller to halt the feed from flow-strand 1.

Table 5. List of components

Component name	Type	Alias	CAS
Vanillylamine hydrochloride	solid	$C_8H_{11}O_2\,N\cdot HCl$	7149-10-2
Nonanoyl chloride	routine	$C_9H_{17}ClO$	764-85-2
Sodium bicarbonate	routine	$NaHCO_3$	144-55-8
Dichloromethane	routine	CH_2Cl_2	75-09-2
Nonivamide	routine	$C_{17}H_{27}NO_3-N_2$	2444-46-4
Sodium chloride	routine	NaCl	7647-14-5
Carbon dioxide	routine	CO_2	124-38-9
Water	routine	H_2O	7732-18-5

Table 6. Physical parameters of the main components

Parameter	**Unit**	$C_9H_{17}ClO$	$C_8H_{12}ClNO_2$	**Nonivamide**
OMEGA		0.55425	0.6791	1.1377
ZC		0.251	0.247	0.216
VC	$cm^3/kmol$	0.5988	0.4422	0.9753
PC	N/m^2	2367380	3689280	1708520
TC	K	678	793	929
TB	K	491.5	566.4	740.6
SG		0.9795	1.1919	1.1514
VLSTD	$cm^3/kmol$	0.18057	0.12865	0.2551
MW		176.68	189.64	293.41

Table 7. Composition of Flow-strand 1

Component	**Quantity**	**(kg/h)**
$C_8H_{12}ClNO_2$	37.9	
$NaHCO_3$	43.3	
CH_2Cl_2	266	
Water	800	
Total	**1147.2**	

Table 8. Composition of Flow-strand 2

Component	**Quantity**	**(kg/h)**
$C_9H_{17}ClO$	35.28	
CH_2Cl_2	266	
Total	**301.28**	

For flow-strand 2, the liquid volume in the reactor acts as a marker for the completion of reactant addition. Once the liquid volume reaches a predetermined level (for the initial reaction, this is 724.24 kg), flow-strand 2 concludes its batch of continuous feeding and ceases further addition. The addition from flow-strand 2 occurs subsequent to the completion of the addition from flow-strand 1.

Throughout the dynamic simulation, samples are collected at intervals of $1, 2, 3, 4, 5$, and 6 hours [23] to analyze flow-strand data and ascertain changes in product concentration over time, as delineated in Table 9.

A linear regression equation, $y = 0.1291x + 0.9819$, is fitted with an adjusted $R^2 = 0.9957$. The intercept is approximately $\frac{1}{[RX]_0} = 1$, and the slope, 0.1291 , represents the reaction rate constant, as depicted in Fig. 7. When comparing the reaction rate constants derived from small-scale experiments and those obtained from RC1e calorimetry scale-up experiments, the dynamic simulation reveals lower reaction rate constants. This discrepancy suggests that the process scale-up affects the reaction rate constants at elevated temperature ranges. Nevertheless, the general trend of concentration changes aligns with the experimental data, affirming the reliability of the experimentally measured reaction kinetics parameters.

3.4. Optimization

3.4.1. Impact of Reactant Feed Molar Ratio

As depicted in Fig. 8, variations in the molar ratio of $C_9H_{17}ClO$ to vanillylamine significantly influence both the reaction rate and the yield of the product, thereby affecting

Table 9. Dynamic simulation of product concentrations over time

Time (h)	0	1	2	3	4	5	6
Product concentration (mol/L)	0	0.8749	0.9366	0.9621	0.9687	0.9748	0.9786

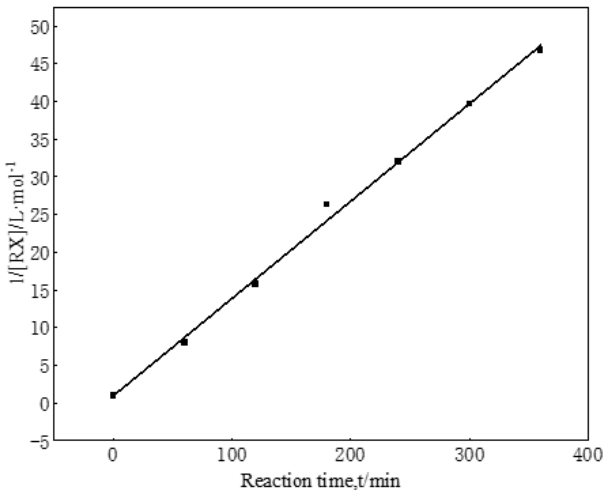

Fig. 7. Dynamic simulation $\frac{1}{[RX]}$ fits the equation with reaction time t

the heat exchange requirements. For rapid exothermic reactions, it is crucial to carefully increase the reactant feed molar ratio while simultaneously considering the safety of the reaction. As the proportion of $C_9H_{17}ClO$ to vanillylamine escalates, there is a continuous increase in the reaction rate. The yield of Nonivamide initially rises, reaching a peak increase of 1.934 percentage points at a molar ratio of 1.1, before subsequently declining. When the feed ratio exceeds 1.1:1, the yield decreases for the following reasons combined with the S_N2 reaction mechanism: first, the excess $C_9H_{17}ClO$ will undergo hydrolysis side reaction in the aqueous phase to generate nonanoic acid, which directly consumes the acylating agent reactant and reduces the effective concentration of the reactant participating in the main reaction; second, the excess $C_9H_{17}ClO$ will accelerate the overall reaction rate, leading to a sudden increase in local heat release of the system and triggering trace side reactions; third, the excess $C_9H_{17}ClO$ will increase the viscosity of the organic phase, reduce the mass transfer efficiency of the liquid-liquid two-phase system, and hinder the contact between the substrate and the nucleophilic reagent in the S_N2 reaction[24]. At a molar ratio of approximately 2, the reaction rate becomes excessively rapid, generating substantial exothermic heat with an adiabatic temperature rise (ΔT) approaching 50°C, thereby reaching a medium level of uncontrolled reaction severity. To ensure the safety of the process, the molar ratio of$C_9H_{17}ClO$ to vanillylamine should be maintained below 2 .

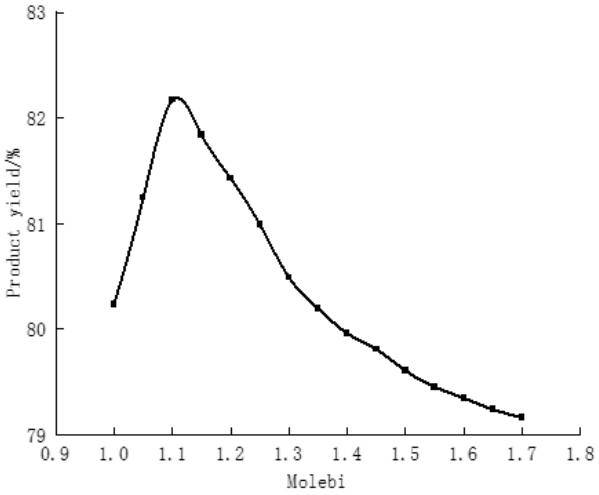

Fig. 8. Variation in the product yield with the molar ratio of the reactant feed

3.4.2. Impact of Feed Temperature

As illustrated in Fig. 9, an increase in the feed temperature of the reactants correlates with a rise in the yield of Nonivamide, alongside increased heat exchange demands. The closer the temperature of the reactants approaches the internal temperature of the reactor, set at 40°C, the more pronounced the change. Given that all reactants are dissolved in CH_2Cl_2 , which has a boiling point of 39.6°C, the optimal maximum feed temperature for reactants is established at 38°C. Within this temperature range, elevating the reactant temperature enhances the initial reaction rate, thereby shortening the time required to reach the reactor's internal temperature of 40°C and reducing the likelihood of side reactions. This adjustment increases the yield of Nonivamide by up to 1.889 percentage points. However, when the temperature of the reactant feed reaches 38°C, further increases would impose a significant additional burden on heat exchange, and the phase change of CH_2Cl_2 precludes further enhancements in Nonivamide yield through temperature modification.

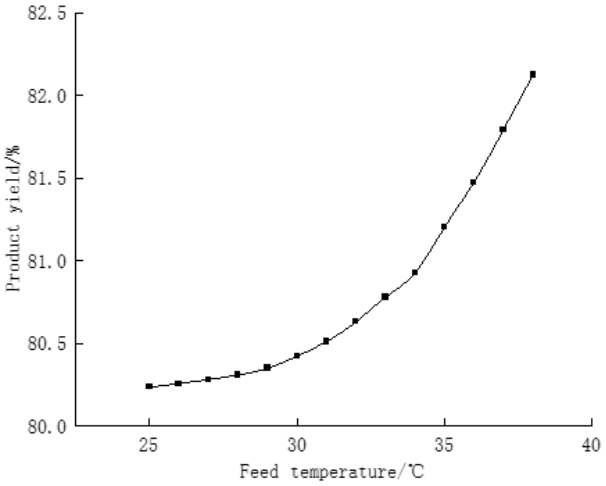

Fig. 9. Variation in the product yield with the feed temperature

3.4.3. Impact of Feed Rate

Upon the addition of $C_8H_{12}ClNO_2$ to the reactor,$C_9H_{17}ClO$ is subsequently introduced. Modulating the feed rate of $C_9H_{17}ClO$ influences the yield of the product. As demonstrated in Fig. 10, in light of the optimized feed temperature results, maintaining $C_9H_{17}ClO$ temperature at 38°C and decreasing its feed rate promotes a more complete reaction, as indicated by an increased product yield. Although the yield gain is modest, peaking at 0.055 percentage points, it is noteworthy. However, sustaining the solution temperature at 38°C for extended periods-near the boiling point of CH_2Cl_2 necessitates advanced process technology support.

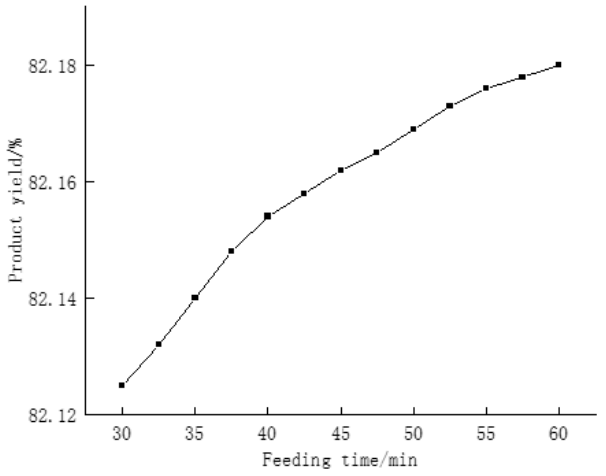

Fig. 10. Variation in the product yield with the feed rate

4. Conclusion

This study has three core innovative points in the research of nonivamide synthesis: first, it is the first to systematically establish the kinetic model of nonivamide liquid-liquid twophase S_N2 reaction and derive the kinetic equation applicable to industrial scale-up; second, it integrates the thermal safety assessment of RC1e calorimeter and the dynamic simulation of Aspen Plus to realize the combination of reaction safety and process optimization; third, it reveals the mass transfer influence law of scale-up of liquid-liquid two-phase rapid exothermic reaction, which provides a reference for the industrial scale-up of similar reactions.

- In laboratory-scale experiments for the synthesis of Nonivamide, it was observed that within certain limits, increasing the quantity of experimental materials does not significantly affect the outcomes. However, as the volume of experimental materials varies, the stirring rate must be maintained at 1300 rpm to mitigate the influence of stirring on the synthesis reaction results.
- The experimental outcomes, combined with reaction kinetics models, have determined that the reaction rate constant for Nonivamide synthesis is $0.1486\,\mathrm{L/(mol \cdot s)}$. The kinetic equation, defined as $k = 34960.37\,e^{\frac{-100911}{RT}}$, provides a robust kinetic foundation essential for the industrial production of Nonivamide. This resolves the lack of theoretical support for the industrial scale-up of Nonivamide synthesis [25].
- Scale-up experiments conducted using the RC1e calorimetric reactor revealed that the molar heat of reaction (ΔH_m) for the Nonivamide synthesis batch reaction at a reactant concentration of 0.2 mol is 249.765 kJ/mol, with an adiabatic temperature rise of $\Delta T = 11.415$. According to industrial safety design criteria, this parameter provides a key basis for the design of cooling systems and safety devices in industrial reactors. These findings are crucial for process safety design and confirm the safety of the reaction process.
- Dynamic simulations were employed to validate the kinetic parameters derived from the Nonivamide synthesis experiments. These simulations also enabled comparison with experimental data to evaluate the effects of process scaling on reaction rates and other relevant parameters, thereby providing a reliable foundation for industrial scale-up and process optimization.
- The influence of variables such as reactant feed molar ratio, feed temperature, and feed rate on product yield

was thoroughly investigated to optimize operational conditions. The optimal conditions were identified as a reactant molar ratio of 1.1 : 1, a feed temperature of 38°C, and a feed duration of 60 min. These conditions increased the product yield by 1.934, 1.889, and 0.055 percentage points, respectively. Applying these optimized parameters in industrial production can achieve a stable yield increase of 3.878 percentage points, maintain the adiabatic temperature rise below 11.415°C, and reduce the cooling system load by approximately 15%. These improvements have significant engineering value for enhancing the production efficiency and safety of Nonivamide.

- **Limitations of this study:** This study only investigated the reaction characteristics of Nonivamide synthesis within the temperature range below 40°C and did not explore reaction kinetics or side-reaction mechanisms at higher temperatures. Industrial scale-up verification was conducted only up to a 2 L RC1e reactor, without pilot-scale verification at the cubic-meter level. Furthermore, the study did not examine the influence of catalysts on reaction rate and yield; future research could investigate catalytic systems suitable for this reaction.

Future research will broaden the temperature range applicable to Nonivamide synthesis reactions, explore the effects of catalysts, examine reaction behaviors at elevated temperatures, quantify mass transfer factors, and validate the reliability of the optimized operational conditions in practical process applications. Additionally, the application of kinetic models in the design of industrial reactors will be further investigated.

References

[1] Q. Zhang, H. Li, S. Zhang, et al., (2025) *"Determination of Nonivamide in guinea pig plasma by high-performance liquid chromatography-tandem mass spectrometry"* **Chinese Journal of Analysis Laboratory *44***(1): 83–88.

[2] J. Zhang, J. Li, X. Deng, et al., (2021) *"Determination of five kinds of capsaicins in edible oil by GPC-UPLC-MS/MS"* **China Oils and Fats *46***(9): 82–86.

[3] Y. Zhang, J. Li, and C. Wang, (2021) *"Scale-up strategy for fast exothermic batch reactions based on reaction calorimetry and dynamic simulation"* **Chemical Engineering Research and Design *176***: 289–301. DOI: 10.1016/j.cherd.2021.08.015.

[4] H. Zhao, W. Zhao, S. Liu, et al., (2022) *"Simultaneous Determination of Octogen and Nonivamide in A New Type of Explosion Suppressant by HPLC"* **Anhui Chemical Industry *48***(5): 102–106.

[5] D. Li, C. Tong, T. Liu, et al., (2024) *"Process simulation and optimization of reaction unit in bisphenol A plant based on Aspen Plus software"* **Petrochemical Technology Application *42***(2): 108–111, 148.

[6] B. Wang, W. Zhao, X. Cao, et al., (2020) *"Determination of Imidazole and Two Impurities in the Imidazole Production Process by HPLC"* **Physical Testing and Chemical Analysis Part B *56***(6): 692–695.

[7] F. Cui, J. Jiang, W. Zhang, et al., (2017) *"Analysis of the Thermal Hazards of the Synthesis Reaction of Tert-butyl Peroxybenzoate"* **China Safety Science Journal *27***(11): 85–90.

[8] Y. Dai, (2017) *"Hardware Composition and Operational Precautions of the RC1e Fully Automatic Reaction Calorimeter"* **Chemical Industry Management** (9): 170–172.

[9] European Process Safety Centre. *Guidelines for Scale-up of Fast Exothermic Batch Reactions*. Tech. rep. EPSC-TR-2020-003. 2020.

[10] Y. Dai, (2017) *"Programming Considerations and Precautions for the RC1e Fully Automatic Reaction Calorimeter"* **Chemical Industry Management** (2): 7–9.

[11] L. Zhang, X. Song, J. Zhang, et al., (2023) *"Study on the Reaction Kinetics of the Isomerization Process of Tranexamic Acid"* **CIESC Journal *74***(10): 4173–4181.

[12] W. Tu, Z. Gan, and D. Zhao, (2015) *"Study on the SN2 Reaction of Haloalkanes"* **Journal of Guangxi Normal University (Natural Science Edition) *32***(3): 50–59.

[13] J. Xie and W. L. Hase, (2016) *"Rethinking the SN2 Reaction"* **Science *352***(6281): 32–33. DOI: 10.1126/science.aaf1531.

[14] H. Liu, X. Chen, and W. Zhang, (2019) *"Scale-up effects on mass transfer and reaction kinetics of fast exothermic liquid-liquid batch reactions"* **Industrial Engineering Chemistry Research *58***(32): 14789–14798. DOI: 10.1021/acs.iecr.9b02567.

[15] C. Zhou. *"The Research and Development of Chemical Engineering Property Estimation System"*. (phdthesis). Qingdao University of Science and Technology, 2022.

[16] X. Wei, L. Yu, J. Jia, et al., (2023) *"Process Simulation and Optimization of the Hydrogen Circulating Desulfurization System in Diesel Hydrodesulfurization Using Aspen Plus"* **Adhesion *50***(4): 125–128.

[17] J. Zhang, W. Wang, F. Liu, et al., (2023) *"ASPEN Simulation of Azeotropic Distillation for Separating Systems Rich in Sec-butyl Acetate Byproducts"* **Adhesion *50***(6): 111–114.

[18] L. Sun. *Process Simulation Training – Aspen HYSYS Tutorial*. China Petrochemical Press, 2019, 424–467.

[19] X. Zhang, (2020) *"Simulation Research of Methanol Distillation Process in Large Coal Chemical Industry"* **Modern Chemical Research** (6): 138–139.

[20] P. Cai, X. Deng, Y. Cao, et al., (2019) *"Incipient Fault Detection of Nonlinear Chemical Processes Based on Weighted Probability Related KPCA"* **Chemical Industry and Engineering Progress *38***(12): 5247–5256.

[21] S. Skogestad, (1997) *"Dynamics and Control of Distillation Columns"* **Chemical Engineering Research and Design *75***(6): 539–562. DOI: 10.1205/026387697524092.

[22] C. Linghu, (2023) *"Application of Aspen HYSYS software in the simulation of low-temperature separation of natural gas"* **Chemical Engineering Design Communications *49***(2): 159–161.

[23] R. Zhang, Z. Liu, J. Wang, et al., (2023) *"Online dynamic simulation and optimization of water-cooled cascade refrigeration systems"* **Chemical Industry and Engineering Progress *42***: 124–132.

[24] J. Chen and W. L. Hase, (2018) *"Dynamics of SN2 reactions in liquid-liquid biphasic systems: A computational and experimental study"* **Journal of Physical Chemistry Letters *9***(12): 3245–3251. DOI: 10.1021/acs.jpclett.8b01243.

[25] K. Schmidt and T. Müller, (2023) *"Industrial-scale synthesis of nonivamide: Process optimization and safety assessment"* **Chemical Engineering Technology *46***(5): 1032–1040. DOI: 10.1002/ceat.202200789.